Divalent Cation Effects on Interactions between Multiple *Arabidopsis* 14-3-3 Isoforms and Phosphopeptide Targets†

Michael S. Manak and Robert J. Ferl*

Program in Plant Molecular and Cellular Biology, Horticultural Sciences, University of Florida, 1143 Hull Road, Fifield Hall 110690, Gainesville, Florida 32611-0690

Received July 6, 2006; Revised Manuscript Received November 8, 2006

ABSTRACT: Oscillations in cellular divalent cation concentrations are key events that can trigger signal transduction cascades. Common cellular divalent cations, such as calcium and magnesium, interact with 14-3-3 proteins. The metal ion interaction causes a conformational change in the 14-3-3 proteins, which is manifested as an increase in hydrophobicity. In this study, the effect of divalent cations on the interaction between 14-3-3 proteins and target peptides was investigated using surface plasmon resonance and isothermal titration calorimetry. The binding between ten recombinant *Arabidopsis* 14-3-3 isoforms and two synthetic target peptides was observed in the presence of various physiologically relevant concentrations of calcium or magnesium, from 1 μM to 1 mM or from 1 μM to 5 mM, respectively. The synthetic target peptides were based on sequences from *Arabidopsis* nitrate reductase (NR2) and the plasma membrane proton pump (AHA2) representing fundamentally different target classes. Isoforms representing every branch of the *Arabidopsis* 14-3-3 phylogenetic tree were tested. The general result for all cases is that an increased concentration of divalent cations in solution causes an increase in the concentration of 14-3-3 protein interacting with the respective phosphopeptide.

Divalent cation concentrations fluctuate among subcellular locations as well as within each location based on plant cell stimuli (*1*−*7*). For example, calcium concentration fluctuates in the cytoplasm upon stimulation by ABA, gibberellin, oxidative signals, red light, circadian rhythm, and heat shock (*6*). Further, magnesium concentration gradients are established in the cell to produce membrane potential between the cytoplasm and the plastids (*7*). Fluctuation in divalent cation levels can cause rapid changes in plant cell protein interaction states (*7*, *8*). For example, calcium-dependent protein kinases (CDPK) are activated upon binding calcium, which causes a conformational change removing the pseudosubstrate domain that inhibits the CDPK from phosphorylating target proteins (*9*, *10*). Many signal transduction events rely on divalent cation levels as mediators of cellular response in addition to general cellular function cues (*6*, *11*). Changes in divalent cation levels can influence 14-3-3/target protein affinities. 14-3-3 proteins interact with phosphorylated target proteins to both modify target proteins' functions and maintain the phosphorylation state within signal transduction cascades connecting cellular communication networks (*12*−*19*).

Early experiments described the binding of divalent cations to *Arabidopsis* 14-3-3 Omega while investigating the sequence comprising the EF-hand-like loop 8 region of isoform Omega (*20*). Experiments designed to answer questions about the requirement of divalent cation presence and the optimal interaction between 14-3-3 proteins and targets followed and included some additional isoforms from the same phylogenetic branch as Omega (*12*, *21*).

Well-studied plant 14-3-3/target protein interactions include proteins such as nitrate reductase (NR2) (*22*−*24*) and the plasma membrane proton pump isoforms (*25*−*31*). Nitrate reductase activity is controlled by a phosphorylation event followed by divalent cation-bound 14-3-3 proteins interacting with the phosphorylated Ser543 of NR2 (*22*, *24*, *32*). Phosphorylated *Arabidopsis* plasma membrane proton pump H^+ATPase (AHA2) and 14-3-3 protein interaction occurs optimally when in the presence of the divalent cation Mg^{2+} (*21*). Therefore, phosphopeptides representing the 14-3-3 target binding site of NR2 and AHA2 were selected as candidates for studying the effects of divalent cations on 14-3-3/phosphopeptide interactions.

Surface plasmon resonance is a proven method for studying 14-3-3 protein/phosphopeptide interaction biochemistry (*33*−*37*). In the present study, a Biacore 3000 (Uppsala, Sweden) was used to evaluate the effects of calcium and magnesium on the interaction between the multiple *Arabidopsis* isoforms and the NR2 and AHA2 phosphopeptides. Select isoform peptide interactions were also examined by isothermal titration. The results show that *Arabidopsis* 14-3-3 proteins increasingly bound to the phosphopeptide surfaces as the concentration of calcium or magnesium ions was increased. These results are consistent with earlier reports concerning the effects of divalent cations on 14-3-3 target interactions (*20*, *22*−*24*, *36*−*38*).

The goal of this investigation was to demonstrate how divalent cations influence 14-3-3/target protein interaction as a means of connecting fluxes in cellular divalent cation levels with 14-3-3 protein involvement with signal trans-

† Support from NSF Grant MCB 0114501 is gratefully acknowledged.

* To whom correspondence should be addressed. Phone: 352-392-1928 ext 301. Fax: 352-392-5653. E-mail: robferl@ufl.edu.

10.1021/bi061366c CCC: $37.00
Published on Web 01/06/2007

duction cascades. In this study, the investigation of the effects exerted by divalent cations on 14-3-3 proteins' interactions was extended to ten isoforms representing all evolutionary branches of the *Arabidopsis* 14-3-3 phylogenetic tree. In addition, a physiologically relevant gradient of divalent cation concentrations (*2*, *3*, *7*) (see Table S1 in Supporting Information) was utilized to suggest the in vivo subcellular locations in which 14-3-3 protein/target interactions may be most likely influenced by divalent cation concentrations.

MATERIALS AND METHODS

Surface Preparation. A CM5 chip was utilized since the epoxyalkanethiol gold-bound dextran surface could be reacted with coupling reagents that covalently bind a phosphopeptide. All surface building steps were performed at a flow rate of 10 μL/min in 20 mM MOPS [3-(*N*-morpholino)propanesulfonic acid], pH 7.5, and 50 mM sodium chloride. The carboxymethyl groups of the dextran layer were reacted with 1-ethyl-3-[3-(dimethylamino)propyl]-carbodiimide (EDC) and *N*-hydroxysuccinimide (NHS) to produce a reactive ester, 4 min injection. The reactive ester was then reacted with 1 M ethylenediamine, pH 8.5, in running buffer for 4 min to produce a stably bound linker and another reactive amine group. The remaining reactive esters were blocked with 1 M ethanolamine, pH 8.5, 4 min injection. The reactive amine of the ethylenediamine was reacted with 100 mM *m*-maleimidobenzoyl-*N*-hydroxysulfosuccinimide ester (Sulfo-MBS; Pierce, Rockford, IL) in 10 mM sodium bicarbonate, pH 8.5, to produce a covalently bound reactive maleimide group, 4 min injection. The maleimide π-bond was reacted with the N-terminal cysteine residue of the phosphopeptide to produce a stable carbon−sulfur bond. The peptide was added at a concentration of 25 μg/mL in 10 mM sodium acetate, pH 5.0, with a 1 min injection. The remaining maleimide groups were blocked with 150 mM L-cysteine in 10 mM sodium acetate, pH 4.0, 10 min injection. A control surface was produced similar to the phosphopeptide surface, except that a cysteine molecule was added at the final step in place of the cysteine-linked phosphopeptide.

Surface Plasmon Resonance Divalent Cation Studies. Recombinant *Arabidopsis* 14-3-3 isoforms were expressed with an amino-terminal 6× histidine tag and purified following the Novagen pET expression system manual (Darmstadt, Germany). Purified recombinant 14-3-3 proteins were dialyzed into running buffer containing 20 mM MOPS, 50 mM NaCl, and 0.005% Tween-20 at pH 7.5. The protein solutions were subjected to ultracentrifugation in a Beckman Coulter, Inc., Optima MAX/MAX-E ultracentrifuge (Fullerton, CA) at 50000*g* for 30 min to ensure only highly soluble protein was in the solution to avoid aggregation on the chip surface. The concentrations of the proteins were measured using the Bio-Rad Bradford assay kit (product number 500-0002) and Smartspec 3000 Bio-Rad (Hercules, CA). Protein purity was considered >95% pure based on Coomassie-stained SDS−PAGE gels (see Figure S1 in Supporting Information). Each isoform was then resuspended to a working concentration of 1.5 μM in running buffer containing either calcium or magnesium at various physiologically relevant concentrations (1 μM to 1 mM or 1 μM to 5 mM, respectively).

Phosphopeptide Synthesis. Peptides were synthesized by soild-phase N^{α}-(9-fluorenylmethoxycarbonyl) (Fmoc) chemistry on an Applied Biosystems synthesizer, model 433A (Foster City, CA), at the University of Florida ICBR protein synthesis core and were purified by HPLC to 99% as determined by mass spectrometry.

Surface Plasmon Resonance Divalent Cation Studies. Each 14-3-3 isoform was first diffused over the control surface and then over the phosphopeptide at a rate of 20 μL/min for 120 s. Then running buffer alone was diffused over the surface causing most of the 14-3-3 protein to dissociate from the phosphopeptide surface. The surfaces were regenerated with 20 mM MOPS, 300 mM NaCl, 200 mM imidazole, 0.1% Tween-20, and 0.03% SDS at a rate of 50 μL/min for 30−60 s. The results of the study were analyzed with Biaevalution software version 4.1 to normalize the start of injection among isoforms as well as zero the baseline at the average when comparing divalent cation concentrations.

Isothermal Titration Calorimetry. A Microcal VP-ITC (isothermal titration calorimeter) (Northampton, MA) was used to measure the interaction between the AHA2 phosphopeptide and 14-3-3 proteins Phi and Kappa. The experiment was conducted at 25 °C. A water reference cell of equal size and shape to the sample cell was used to determine the amount of energy exchanged with the surroundings when the two molecules of interest interact. Purified recombinant 14-3-3 protein was placed in the sample cell reservoir at a concentration of 8.25 μM in a total volume of 1.8 mL (20 mM MOPS, 50 mM NaCl, and 0.005% Tween-20 at pH 7.5 with either 10 mM EDTA or 55 mM $MgCl_2$). Synthetic phosphopeptide was placed in the syringe at a concentration of 230 μM in 20 mM MOPS, 50 mM NaCl, and 0.005% Tween-20 at pH 7.5 with either 10 mM EDTA or 55 mM $MgCl_2$. The reference cell temperature was set at 25 °C. The phosphopeptide was injected into the protein solution at 3 μL per injection for a total of 50 injections. The final overall protein/peptide solution volume was 1.95 mL. Upon collecting the data a 1 to 1 interaction model was fit to the data using a Levenberg−Marquardt equation within the Origin 7.1 software package (Northampton, MA) to derive the enthalpy, equilibrium affinity constants, entropy, and stoichiometric ratio of peptide to protein. The data were fit to the derived curve based on molecular interaction principles and reducing the difference between the model and the raw data as measured by the resulting Chi-squared value.

RESULTS

Basic Experimental Arrangement. Recombinant 14-3-3 proteins were used in the investigation to ensure that large enough pools of consistent sample protein were available for use throughout the investigation. Accurate results require a homogeneous interaction surface; therefore, synthetically derived phosphopeptides were used to ensure that the peptides were uniformly phosphorylated and highly purified. The recombinant 14-3-3 proteins (cDNA accession numbers: Omega, M96855; Chi L09112; Phi, L09111; Psi, L09110; Nu, U60445; Upsilon, L09109; Kappa, U36447; Lambda, U68545; Epsilon, U36446; Mu, U60444) (*39*−*42*) and the phosphopeptide target binding sites of NR2 and AHA2 were based on *Arabidopsis* protein sequences. The recombinant proteins were produced as described in Materials

Table 1: Consensus Target Sequences and Representative Phosphopeptides Used within the Experimental System

consensus sequence type	consensus sequence	peptide studied
mode 1	R/KXXpS/TXP[a]	C-SLKKSVpSTPFMN
mode 2	R/KXXXpS/TXP	
mode 3	YpTV[b]	C-KLKGLDIETPSHYpTV

[a] pS indicates the serine residue is phosphorylated. [b] pT indicates the threonine residue is phosphorylated.

and Methods based on the exact cDNAs derived in the listed citations (*39*−*42*). The NR2 (gene identification number AT1G37130.1) phosphopeptide represents both the mode 1 (R/KxxpS/TxP) and mode 2 (R/KxxxpS/TxP) consensus sequences (*33*, *34*) (Table 1). The AHA2 (gene identification number AT4G30190.1) phosphopeptide represents the mode 3 (YpTV) consensus sequence found on the carboxyl terminal autoinhibitory domain of the H^+ATPase family (Table 1) (*30*). An amino-terminal cysteine residue was added to each phosphopeptide as a linker and is not part of the native sequence. The peptides were designed to represent the natural location of the phosphorylated group. In the case of NR2 the phosphoserine was within the peptide sequence, whereas the phosphothreonine of the AHA2 peptide was located at the penultimate residue of the carboxyl terminus. Control surface plasmon resonance spectroscopy experiments demonstrated that neither calcium nor magnesium alone showed a detectable interaction with the bound phosphopeptides and that the presence of the 6× histidine tag had a negligible effect on 14-3-3 interaction with the bound peptides (data not shown). In addition, isothermal titration calorimetry was used to examine selected 14-3-3 interactions of phosphopeptide targets in relevant concentrations of divalent.

Effects of Calcium Concentration on the Interaction between 14-3-3 Proteins and the AHA2 Phosphopeptides. Surface plasmon resonance spectroscopy was used to monitor the interactions of recombinant 14-3-3 proteins and target phosphopeptides with 14-3-3 proteins as the analyte and the phosphopeptides as a coupled ligand (see Materials and Methods section for protein and phosphopeptide synthesis details). Panels A−D of Figure 1 illustrate association and dissociation curves for Omega, Epsilon, Lambda, and Nu (each representing one of the major *Arabidopsis* 14-3-3 family phylogenetic subgroups) interacting with the AHA2 phosphopeptide in the presence of various calcium concentrations. The phylogenetic tree of *Arabidopsis* 14-3-3 proteins contains a number of major branches, some of which are very deeply rooted (see Figure S2 in Supporting Information), illustrating the importance of capturing the range of diversity within the *Arabidopsis* 14-3-3 protein family. Each of the four isoforms in Figure 1 increased in binding as the concentration of calcium increased. As the concentration of calcium was increased, the concentration of 14-3-3 protein bound to the H^+ATPase surface increased, which signifies that the calcium concentration was an important component affecting each of the isoforms interacting with the AHA2 phosphopeptide surface. When comparing each concentration of calcium, the overall shape of the curves for each isoform indicates that the association rate was more affected by the increase in cation concentration than the dissociation rates.

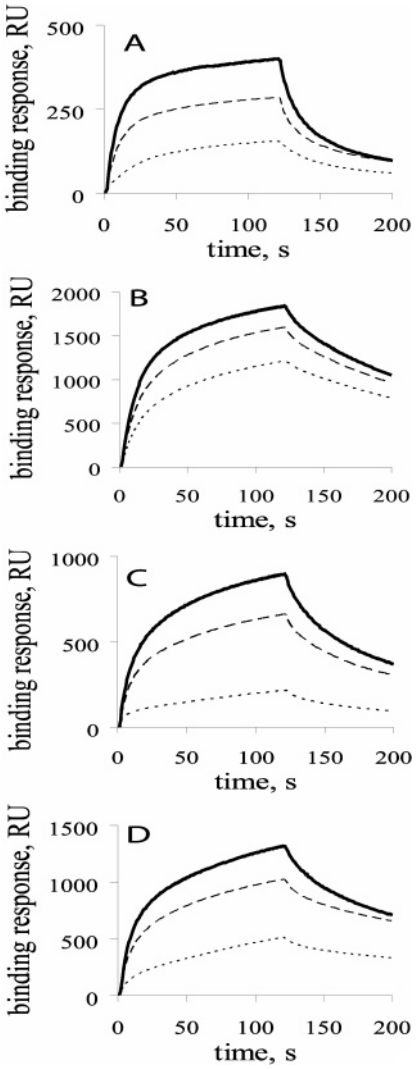

FIGURE 1: Sensorgrams of surface plasmon resonance spectroscopy depicting the 14-3-3 isoforms (A) Omega, (B) Epsilon, (C) Lambda, and (D) Nu interacting with the AHA2 phosphopeptide with various calcium concentrations: 1 μM (•••), 500 μM (− −), 1000 μM (—). A flow rate of 20 μL/min was used for each isoform. After each isoform was investigated, the surface was regenerated to produce a surface with a baseline equivalent to the starting baseline. Data shown were background subtracted for control surface response levels pertaining to each isoform.

Response levels of all ten isoforms tested are shown in Table 2. Each of these isoforms displayed a profile of increased binding to the AHA2 phosphopeptide surface similar to the isoforms shown in Figure 1 (see Supporting Information). Experiments conducted in the presence of 10 mM EDTA affirm that calcium ions were responsible for the positive binding effects observed for each isoform in Table 2. The EDTA experiment demonstrates two aspects about 14-3-3 protein/AHA2 phosphopeptide interaction: first, that a basal level of interaction occurred between the 14-3-3 proteins and the phosphopeptide without calcium freely available in solution, and second, that calcium increased the concentration of 14-3-3 proteins bound to the phosphopeptide surface above the basal level.

Effects of Magnesium Concentration on the Interaction between 14-3-3 Proteins and the AHA2 Phosphopeptide. Magnesium concentrations were investigated in a similar fashion to the calcium concentration experiments for their influence on interaction between the various 14-3-3 isoforms

Table 2: Maximum Binding Response Levels for 14-3-3 Isoforms Interacting with the AHA2 Phosphopeptide under Various Calcium and Magnesium Concentrations

	Mu (RU)[a]	Psi (RU)	Omega (RU)	Chi (RU)	Upsilon (RU)	Kappa (RU)	Lambda (RU)	Phi (RU)	Nu (RU)	Epsilon (RU)
[Ca] (μM)										
1000	123[b] ± 16[c]	296 ± 71	399 ± 14	553 ± 21	537 ± 39	788 ± 23	898 ± 25	1186 ± 31	1317 ± 105	1842 ± 33
500	270 ± 12	228 ± 47	285 ± 9	326 ± 7	422 ± 24	610 ± 14	662 ± 20	997 ± 34	1026 ± 2	1600 ± 30
1	206 ± 11	213 ± 59	156 ± 8	141 ± 11	234 ± 47	ND	217 ± 59	421 ± 165	511 ± 2	1212 ± 20
0.1	159 ± 10	4 ± 0.2	138 ± 8	71 ± 9	136 ± 16	155 ± 9	61 ± 3	134 ± 9	322 ± 12	339 ± 11
EDTA, 10 mM	109 ± 3	3 ± 0.2	134 ± 5	84 ± 2	183 ± 17	119 ± 4	78 ± 6	110 ± 4	288 ± 21	263 ± 24
[Mg] (μM)										
5000	542 ± 14	ND	897 ± 25	1725 ± 36	1123 ± 30	1437 ± 29	1648 ± 32	1886 ± 42	2178 ± 22	2330 ± 29
1000	175 ± 13	ND	257 ± 10	354 ± 8	310 ± 22	587 ± 2	607 ± 18	869 ± 32	977 ± 2	1592 ± 27
500	161 ± 8	ND	226 ± 11	295 ± 10	340 ± 40	469 ± 1	533 ± 15	774 ± 26	835 ± 1	1507 ± 27
1	131 ± 11	ND	125 ± 7	124 ± 17	192 ± 14	241 ± 1	226 ± 64	339 ± 77	516 ± 2	1188 ± 26
EDTA,[d] 10 mM	72 ± 6	ND	135 ± 5	84 ± 4	184 ± 18	123 ± 7	79 ± 5	60 ± 10	302 ± 1	247 ± 20

[a] RU, response units. [b] Mean measure, $n = 3$. [c] 95% confidence interval. [d] EDTA data from the magnesium-influenced set of experiments.

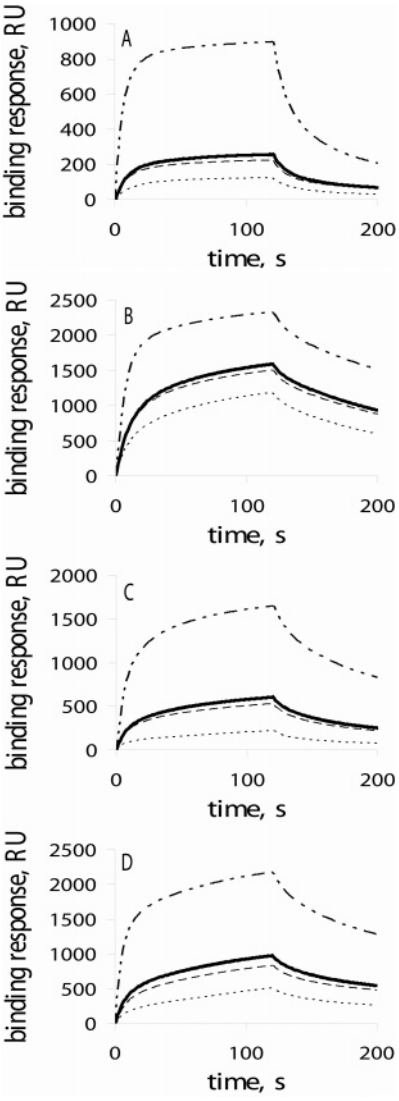

FIGURE 2: Sensorgrams of surface plasmon resonance spectroscopy depicting the 14-3-3 isoforms (A) Omega, (B) Epsilon, (C) Lambda, and (D) Nu interacting with the AHA2 phosphopeptide with various magnesium concentrations: 1 μM (•••), 500 μM (− −), 1000 μM (—), and 5000 μM (•—•). A flow rate of 20 μL/min was used for each isoform. After each isoform was investigated, the surface was regenerated to produce a surface with a baseline equivalent to the starting baseline. Data shown were background subtracted for control surface response levels pertaining to each isoform.

and the AHA2 phosphopeptide. Data shown in Figure 2 and summarized in Table 2 demonstrate that increasing magnesium concentrations increases the level of each 14-3-3 isoform bound to the AHA2 peptide. This result indicates that magnesium has an effect comparable to that of calcium on 14-3-3 proteins interacting with the AHA2 peptide. A significant increase in binding response occurs when the proteins are exposed to a 5 mM magnesium concentration compared to the lower three magnesium concentrations investigated. The binding curves for the magnesium interaction studies showed that the association rate was more affected by increased magnesium concentration than the dissociation rate, since the association portion of the curves differed more than the dissociation rate portion of the curves. The remaining results for the other isoforms listed in Table 2 indicated that these isoforms behaved similarly with regard to levels of magnesium and relative binding response. All of the free magnesium levels increased the amount of 14-3-3 protein bound to the phosphopeptide surface relative to experiments including 10 mM EDTA (Table 2).

The significant increase in protein binding response observed during the 5 mM magnesium experiment relative to the lower concentrations prompted a second set of experiments designed to observe the effects of high physiologically relevant concentrations of magnesium on 14-3-3 protein/phosphopeptide interactions. Another surface was built using the AHA2 phosphopeptide. Results indicated that a second significant increase in phosphopeptide surface/14-3-3 protein interaction occurred when 100 mM magnesium was included in solution relative to 5 or 10 mM magnesium (see Figure S4 in Supporting Information).

Effects of Calcium Concentration on the Interaction between 14-3-3 Proteins and the NR2 Phosphopeptides. NR2 phosphopeptide 14-3-3 protein interaction studies were performed as a comparison to the AHA2 phosphopeptide interaction studies on effects of the divalent cations. Increased calcium concentration caused increased binding of the 14-3-3 isoforms to the NR2 phosphopeptide surface in general (Table 3 for summary data; see Supporting Information for sensorgrams). Isoform Omega increased in binding when calcium levels increased from 1 to 500 or 1000 μM but did not significantly increase in binding when calcium increased from 500 to 1000 μM. Results from isoform Psi and Mu investigations produced similar response-curve results to isoform Omega. Isoform Chi and Upsilon studies show that increased concentrations of calcium from 1 to 500 or 1000 μM increased 14-3-3 protein binding. Regardless of the isoform investigated, the binding curves demonstrated that

Table 3: Maximum Binding Response Levels for 14-3-3 Isoforms Interacting with the NR2 Phosphopeptide under Various Calcium and Magnesium Concentrations

	Chi (RU)[a]	Epsilon (RU)	Kappa (RU)	Lambda (RU)	Mu (RU)	Nu (RU)	Omega (RU)	Phi (RU)	Psi (RU)	Upsilon (RU)
[Ca] (μM)										
1000	59[b] ± 2[c]	352 ± 7	63 ± 5	158 ± 34	119 ± 7	154 ± 50	90 ± 6	204 ± 8	347 ± 11	104 ± 29
500	68 ± 4	154 ± 25	66 ± 2	117 ± 5	114 ± 3	101 ± 2	85 ± 2	130 ± 4	344 ± 24	130 ± 3
1	48 ± 2	109 ± 5	48 ± 1	75 ± 2	96 ± 2	67 ± 2	60 ± 1	63 ± 7	22 ± 1	91 ± 19
EDTA, 10 mM	1 ± 1	1 ± 1	1 ± 1	0	0	8 ± 1	0	0	3 ± 1	0
[Mg] (μM)										
1000	47 ± 2	157 ± 7	44 ± 2	90 ± 5	105 ± 3	71 ± 2	69 ± 2	82 ± 9	21 ± 1	93 ± 2
500	48 ± 1	114 ± 19	35 ± 2	77 ± 2	92 ± 2	63 ± 2	61 ± 2	85 ± 3	15 ± 1	79 ± 2
1	49 ± 1	109 ± 4	49 ± 1	75 ± 1	96 ± 2	68 ± 1	61 ± 1	62 ± 5	19 ± 1	92 ± 2
EDTA,[d] 10 mM	0	2 ± 1	1 ± 1	0	0	8 ± 1	0	0	0	0

[a] RU, response units. [b] Mean measure, $n = 3$. [c] 95% confidence interval. [d] EDTA data from the magnesium-influenced set of experiments.

the association rate was more affected by calcium concentration than dissociation rate (see Supporting Information for sensorgrams), which results in a general increase in binding when comparing 1 to 500 or 1000 μM.

Effects of Magnesium Concentration on the Interaction between 14-3-3 Proteins and the NR2 Phosphopeptides. Magnesium concentrations were also investigated in order to extend the range of isoform results reported in response to the magnesium ion and compare results to AHA2 phosphopeptide studies. When observing specific isoform response curves such as those for Omega, Lambda, Nu, and Chi, the increased magnesium concentrations have a reduced effect on the overall level of binding to the NR2 phosphopeptide compared to results obtained for the same isoforms interacting with the AHA2 phosphopeptide in the presence of varying magnesium concentrations (Table 3; see Supporting Information, Figures S3 and S5). For example, isoform Nu increased binding to the AHA2 phosphopeptide by 142 response units when the concentration of magnesium was increased from 500 to 1000 μM, whereas isoform Nu binding increased by 8 response units to the NR2 phosphopeptide when the magnesium concentration was increased from 500 to 1000 μM.

The magnesium concentration directly affected the concentration of each of the 14-3-3 proteins bound to the NR2 phosphopeptide surface. Isoform Phi (Table 3) increased in binding response when the magnesium concentration increased from 1 to 500 or 1000 μM. The experiments with isoform Kappa demonstrate that binding response was negatively affected by increased magnesium concentrations from 1 to 500 μM yet positively affected by increased magnesium concentrations from 500 to 1000 μM. Upsilon isoform showed little difference in response level between 1 and 500 or 1000 μM yet confirmed no binding in the presence of EDTA (Table 3). Response levels for isoforms Psi and Mu were more positively affected by magnesium concentrations of 1000 μM compared to 1 or 500 μM, whereas magnesium concentrations of 500 μM negatively affected Psi and Mu response levels compared to 1 or 1000 μM (Table 3). Throughout all of the investigations for each isoform, it was clear that both calcium and magnesium concentrations influenced the levels of interaction between 14-3-3 proteins and target phosphopeptides.

Effects of Magnesium versus EDTA on the Interaction between 14-3-3 Proteins and the AHA2 Phosphopeptides Measured by Isothermal Titration Calorimetry. In order to supplement and confirm the results of the surface plasmon resonance data, isothermal titration calorimetry (ITC) was used to measure the interactions between 14-3-3 isoforms with the AHA2 phosphopeptide in the presence of magnesium or EDTA. Phi and Kappa were selected as representative isoforms since these two isoforms represent the divergent members of the *Arabidopsis* 14-3-3 protein family (see Supporting Information, Figure S2). Interactions between isoform Phi and the AHA2 phosphopeptide in the presence of 10 mM EDTA showed no significant change in the amount of thermal energy exchanged with the surrounding environment over time, which indicates no interaction occurring between isoform Phi and the AHA2 phosphopeptide in the presence of EDTA (Figure 3A,B). Results from ITC experiments measuring the Kappa and AHA2 phosphopeptide interactions in the presence of EDTA were similar to the results of the Phi and AHA2 phosphopeptide interactions (Figure 4A,B). Results of both Phi and Kappa isoforms interacting with the AHA2 phosphopeptide in the presence of 5 mM $MgCl_2$ produced measurable changes in the thermal energy exchanged with the surrounding environment (Figures 3C,D and 4C,D). The affinity (equilibrium dissociation constant, K_D) of the two isoforms for the AHA2 phosphopeptide in the presence of 5 mM $MgCl_2$ was 30.1 ± 17 nM (95% confidence interval) and 123.8 ± 39.1 nM (95% confidence interval) for Phi and Kappa, respectively. The results of the ITC experiment demonstrate that lack of divalent cations available in solution prevents the interaction of either Phi or Kappa with the AHA2 phosphopeptide and that interaction occurs between Phi or Kappa and the AHA2 phosphopeptide when 55 mM $MgCl_2$ was available in the interaction environment. Additionally, the two isoforms have a different affinity for the same phosphopeptide target, signifying the diversity among the *Arabidopsis* 14-3-3 isoforms.

DISCUSSION

Surface plasmon resonance spectroscopy results indicated that the concentration of divalent cation and the type of divalent cation both influence the interaction between 14-3-3 proteins and the two phosphopeptide surfaces tested. These results correlate with previous experiments in that the increase in divalent cation increased 14-3-3 protein and phosphopeptide interaction (*12*, *22*−*24*). Results from the ITC experiments demonstrated that divalent cations are an integral element involved in the 14-3-3 protein AHA2 phosphopeptide interactions. The effects of divalent cations have not been previously reported for isoforms Lambda,

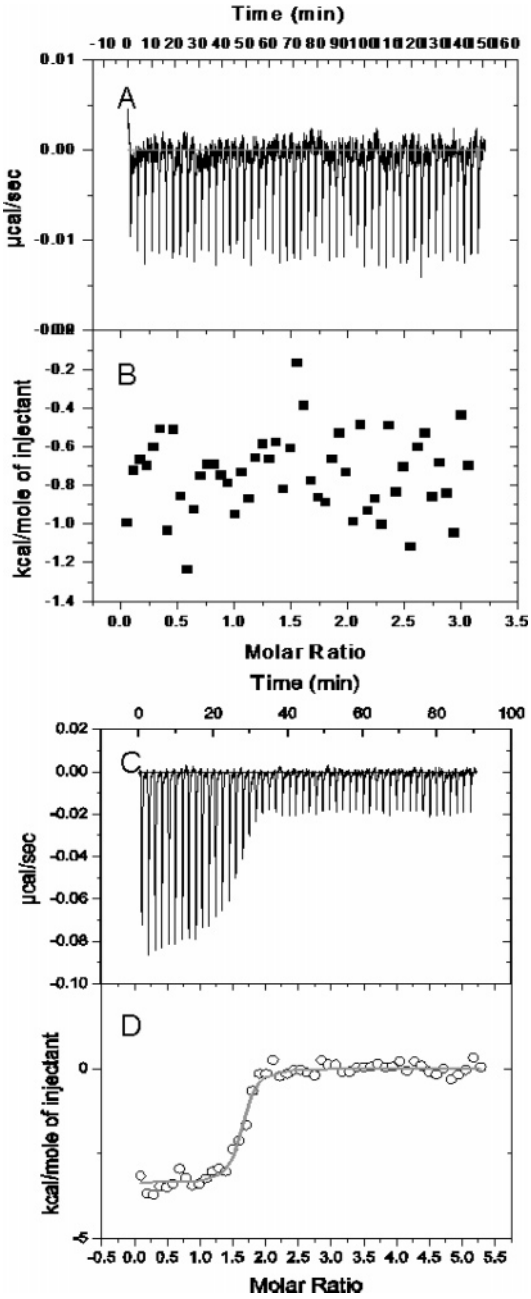

FIGURE 3: Phi/AHA2 interaction data from ITC. (A) No enthalpy change in the system occurred based on Phi and the AHA2 phosphopeptide interacting in a 10 mM EDTA solution. (B) No data fit was possible since no measurable interaction occurred between Phi and the AHA2 phosphopeptide in a 10 mM EDTA solution. (C) Enthalpy change in the system caused upon Phi/AHA2 exothermic interaction plotted as the amount of power required per second to maintain the sample cell and reference cell at the same temperature on the ordinate axis against the molar ratio of 14-3-3 dimer per peptide on the abscissa. (D) Data fit to a 1 to 1 interaction model using a Levenberg−Marquardt equation. Each data point was plotted as the amount of enthalpy change per mole of injected peptide on the ordinate axis against the molar ratio of 14-3-3 dimer per peptide on the abscissa. The line is the curve fitting the data. The black circles are the raw data points.

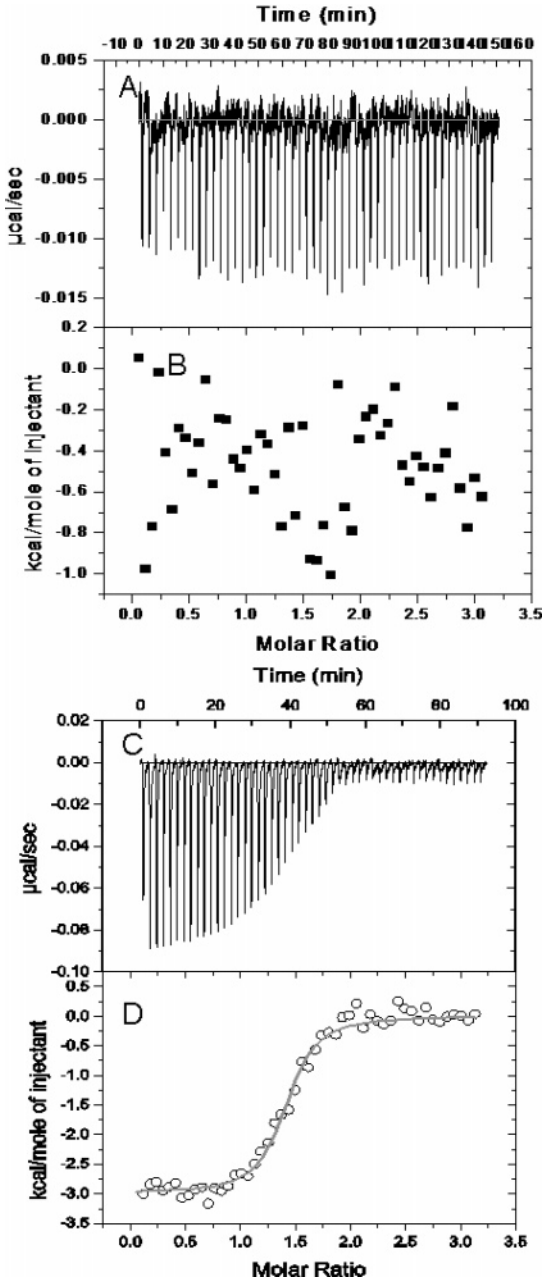

FIGURE 4: Kappa/AHA2 interaction data from ITC. (A) No enthalpy change in the system occurred based on Kappa and the AHA2 phosphopeptide interacting in a 10 mM EDTA solution. (B) No data fit was possible since no measurable interaction occurred between Kappa and the AHA2 phosphopeptide in a 10 mM EDTA solution. (C) Enthalpy change in the system caused upon Kappa/AHA2 exothermic interaction plotted as the amount of power required per second to maintain the sample cell and reference cell at the same temperature on the ordinate axis against the molar ratio of 14-3-3 dimer per peptide on the abscissa. (D) Data fit to a 1 to 1 interaction model using a Levenberg−Marquardt equation. Each data point was plotted as the amount of enthalpy change per mole of injected peptide on the ordinate axis against the molar ratio of 14-3-3 dimer per peptide on the abscissa. The line is the curve fitting the data. The black circles are the raw data points.

Kappa, Nu, Upsilon, Psi, Epsilon, or Mu. Data summarized in Tables 2 and 3 demonstrated that there was an increase in binding for each of the isoforms when the concentration of calcium was increased from 1 to 500 μM. There also was an increase in binding when the calcium concentration was elevated from 500 to 1000 μM. The magnitude of the increase in binding to AHA2 was different among isoforms when various concentrations of divalent cations were applied. For example, increasing the calcium concentration from 1 or 1000 μM elicited a 2.6-fold change in isoform Omega/AHA2 phosphopeptide interaction level, compared to a 1.5-fold change with Epsilon and AHA2 (Figure 1A,B). The same trend follows when comparing Omega and Epsilon

differences in AHA2 phosphopeptide interaction level between magnesium concentrations of 1 and 1000 μM; Omega binding increased 2.0-fold while to Epsilon binding increased 1.3-fold (Figure 2A,B).

The differences in the carboxyl-terminal sequences of the 14-3-3 isoforms may contribute to the different interaction effects observed among the isoforms. Experiments investigating the carboxyl terminus of isoform Omega suggest that when the EF-hand-like loop 8 region binds a divalent cation, the carboxyl terminus forms a tenth α-helix (*43*). Furthermore, formation of the carboxyl terminus into a tenth α-helix is thought to remove the carboxyl terminus from occupying the amphipathic groove in which target peptides bind (*43*−*46*). Thus the differences in cation effect among isoforms may be due to the differential action of their carboxyl termini.

The investigation currently under discussion focuses on multiple isoforms from each subgroup of the *Arabidopsis* phylogenetic tree. This approach highlights comparisons among isoforms to elucidate isoform-specific effects divalent cations could have on 14-3-3 protein/target interactions. Kappa and Lambda binding to the AHA2 phosphopeptide surface were most highly affected by the increasing concentrations of calcium or magnesium. Omega, Phi, and Chi were the second most affected group by increasing concentrations of calcium or magnesium, again while interacting with the AHA2 phosphopeptide. The Epsilon and Mu group was the third most affected, and the Psi, Upsilon, and Nu group was the least affected by the increase in calcium or magnesium concentrations when interacting with AHA2 (Table 2). Thus cation effects on the interaction with the AHA2 peptide seem grouped by phylogenetic relatedness. The ITC data support the general trend that *Arabidopsis* 14-3-3 isoforms require divalent cations in order to interact with the AHA2 phosphopeptide optimally (Figures 3 and 4).

In contrast, the Epsilon and Mu group was the most affected by the increase in either calcium or magnesium when interacting with the NR2 phosphopeptide, while the Omega, Phi, and Chi group was second most affected. The Psi, Upsilon, and Nu group and the Kappa and Lambda group were the least affected by the increase in calcium or magnesium when interacting with the NR2 phosphopeptide surface (Table 3). Thus cation effects on the interaction with the NR2 phosphopeptide are also grouped along phylogenetic lines, but the relationships are not in the same hierarchical order as the AHA2 effects.

Eukaryotes by definition have compartmentalized organelles that are responsible for specific functions. Each of the organelles and their respective membranes cause cells to develop gradients of both energy and information potential. As members of signal transduction cascades, 14-3-3 proteins help to connect the energy and information flow both intra- and extracellularly (*12*, *13*, *19*, *26*, *27*, *29*, *47*). Divalent cation concentrations fluctuate within the plant (summarized in Table S1 of Supporting Information) depending on subcellular location or response to stimuli. For example, exposure to ABA can cause cytosolic calcium levels to rise above 1 μM (*1*), a level that had clear influences on 14-3-3 protein target interaction (Figure 2 and Supporting Information). Additionally, when root hair development occurs, cytosolic levels of calcium fluctuate from 50 to 700 nM (*48*). In contrast, cytosolic magnesium levels average 5 mM and can oscillate as high as 10 mM (see Table S1 in Supporting Information). An increase in available magnesium concentration had a positive influence on the concentration of 14-3-3 protein bound to the AHA2 phosphopeptide. The plasma membrane and vacuolar proton pump and the SV-channel proteins are regulated by 14-3-3 proteins, implying that the balance among cytosolic proton, calcium, and magnesium levels may be partially controlled by 14-3-3 proteins interacting with the respective membrane proteins responsible for allowing calcium and protons levels to fluctuate.

In addition to divalent cations, other physiological signals influence 14-3-3 protein/target interactions such as pH, polyamines, and adenosine 5′-monophosphate (5′-AMP) (*23*, *37*). Lowering the pH from 7.5 to 6.5 causes increases in 14-3-3 protein target binding similar to increases seen when divalent cation concentrations are raised to 5 mM (*37*). Polyamines also affect 14-3-3 protein/target peptide interaction levels with a profile similar to increased divalent cation concentrations. The mode of action is actually similar as both polyamines and divalent cations bind within the loop 8 region of 14-3-3 proteins (*36*). The addition of 5′-AMP to solutions containing 14-3-3 proteins and targets disrupts 14-3-3 protein and target interactions (*38*). An analogue to 5′-AMP, ZMP, can be used to disrupt 14-3-3 protein and target interactions, an effect that has been demonstrated biochemically (*36*) and in vivo through the differential localization of 14-3-3 proteins before and after treatment with the 5′-AMP analogue (*49*). Taken together, it is clear that 14-3-3 protein/target interactions are affected by several physiological cues in addition to divalent cations. The fluctuating concentration of each of these cues in concert with divalent cations could drive the signal transduction cascades involving 14-3-3 proteins at key points within cellular communication networks.

Current theory places the metal binding domain in loop 8 between α-helices 8 and 9 (*12*, *20*, *23*, *36*, *38*, *43*). The crystal structure of a human 14-3-3 isoform Sigma (PDB code: 1YWT) has a calcium atom coordinated with a histidine molecule located at the end of the fourth α-helix (*56*). The Sigma isoform histidine molecule that is coordinated with the calcium atom is conserved in all of the *Arabidopsis* isoforms except Omega, Chi, and Phi. The coordination of the calcium atom with the fourth-helix histidine may represent a second and/or alternative metal binding site in the 14-3-3 protein family. The existence of a second or alternative metal binding site outside of the loop 8 EF-hand metal binding site could increase 14-3-3 proteins' ability to participate in signal transduction events governed by fluctuations in cellular divalent cation concentrations as well as expand the role divalent cations play as 14-3-3 protein cofactors.

There are differences in the effects of calcium versus magnesium (Tables 2 and 3). For example, when comparing isoform Omega's response level in the presence of 500 μM calcium, the maximum response level reached approximately 400 RU, whereas in the presence of magnesium the maximum level was approximately 200 RU. Lu et al. demonstrated that the *Arabidopsis* isoform Omega binds calcium with an affinity of 550 μM and within the same study showed that magnesium is outcompeted by calcium for binding to the EF-hand-like region loop 8 (*20*). The observation that calcium binds the loop 8 region with higher affinity than magnesium is consistent with observations

reported for other EF-hand motifs (*50*, *51*). The mechanism governing 14-3-3 target interaction was strongly influenced by magnesium in solution, a common feature of both EF-hand-containing kinases and phosphatases. EF-hand-containing proteins can bind calcium and magnesium with an affinity of 0.05 and 200 μM, respectively (*51*). Therefore, EF-hand-containing phosphatases such as protein phosphatase 2C could compete with 14-3-3 proteins for available calcium or magnesium, which could disrupt 14-3-3 protein/target interaction freeing the target protein phosphate for phosphatase enzymatic action. In this model, the target protein would no longer interact with the 14-3-3 protein, thereby disrupting the signal conveyed by the act of 14-3-3 protein binding and the phosphate would be free for recycling into the phosphate pool.

An inspection of the *Arabidopsis* protein sequences shows similar amino acids responsible for the coordinating metal. Differences in other positions along the sequence are observable that may contribute to isoform-specific differences in phosphopeptide interaction. Sinnige et al. demonstrated that a single amino acid change within the EF-hand-like region of barley 14-3-3 proteins directly affected the ability of a 14-3-3 isoform to interact with a NR2 phosphopeptide independent of calcium or magnesium availability in solution (*52*). In another study, proteolytic protection assays were used to monitor the differences between isoforms when divalent cations were present, demonstrating that the different isoforms were more likely to become digested based on increased flexibility due to difference in the metal binding domain (*53*). Coupling the proteolytic protection assays with a mutation analysis showed that a single amino acid change (asparagine 213 to glycine) within the metal binding domain of isoform Mu caused an increase in protein flexibility and cleavage similar to isoform Omega, where a glycine at position 213 is its natural state (*53*). In both the barley 14-3-3 experiments and the proteolytic protection assays, amino acids which are not directly responsible for coordinating divalent cations were mutated within the metal binding region. These mutations caused a change in the level of interaction with targets, yet did not negatively affect metal binding to the 14-3-3 protein. These data are in agreement with the findings of the current study in that the concentrations of Mu and Epsilon bound to phosphopeptide surfaces were affected by divalent cation concentration similarly to the other *Arabidopsis* isoforms such as Omega.

In conclusion, the interaction response of each of the *Arabidopsis* 14-3-3 isoforms investigated was generally enhanced by the addition of either calcium or magnesium, with calcium having a greater effect than magnesium. The result of the differences among each isoform interaction with each of the phosphopeptides may reflect differences in the capacity of each isoform to bind calcium or magnesium as well as highlight the differences in 14-3-3 carboxyl-terminal sequences. Observations collected within this study provide evidence that *Arabidopsis* 14-3-3 isoforms both generally and uniquely respond to calcium and magnesium levels and support the concept that the differences among isoforms have an impact on *Arabidopsis* 14-3-3 protein/target phosphopeptide interaction. Engineering the 14-3-3 EF-hand-like region to respond differently to calcium or magnesium could lead to interesting biological results as well as potential opportunities for biotechnologically oriented control over 14-3-3 protein signal transduction pathway points.

ACKNOWLEDGMENT

The authors thank Alfred Chung for synthesizing the phosphopeptides and Marjorie Chow and Kevin Kroll for assistance in using the Biacore 3000. The authors also thank Paul Sehnke for technical advice on recombinant 14-3-3 protein expression as well as for scientific discussion pertaining to experimental design. Finally, the authors thank Anna-Lisa Paul for thorough reading of the manuscript and advice given therein.

SUPPORTING INFORMATION AVAILABLE

Six figures and one table as described in the text. This material is available free of charge via the Internet at http://pubs.acs.org.

REFERENCES

1. Allen, G. J., Kwak, J. M., Chu, S. P., Llopis, J., Tsien, R. Y., Harper, J. F., and Schroeder, J. I. (1999) Cameleon calcium indicator reports cytoplasmic calcium dynamics in *Arabidopsis* guard cells, *Plant J. 19*, 735−747.
2. Gilroy, S., Bethke, P. C., and Jones, R. L. (1993) Calcium homeostasis in plants, *J. Cell Sci. 106* (Part 2), 453−461.
3. Gilroy, S., and Trewavas, A. (2001) Signal processing and transduction in plant cells: the end of the beginning?, *Nat. Rev. Mol. Cell Biol. 2*, 307−314.
4. Igamberdiev, A. U., and Kleczkowski, L. A. (2001) Implications of adenylate kinase-governed equilibrium of adenylates on contents of free magnesium in plant cells and compartments, *Biochem. J. 360*, 225−231.
5. Igamberdiev, A. U., and Kleczkowski, L. A. (2003) Membrane potential, adenylate levels and Mg^{2+} are interconnected via adenylate kinase equilibrium in plant cells, *Biochim. Biophys. Acta 1607*, 111−119.
6. Sanders, D., Brownlee, C., and Harper, J. F. (1999) Communicating with calcium, *Plant Cell 11*, 691−706.
7. Shaul, O. (2002) Magnesium transport and function in plants: the tip of the iceberg, *Biometals 15*, 309−323.
8. Yang, T., Chaudhuri, S., Yang, L., Chen, Y., and Poovaiah, B. W. (2004) Calcium/calmodulin up-regulates a cytoplasmic receptor-like kinase in plants, *J. Biol. Chem. 279*, 42552−42559.
9. Harmon, A. C., Yoo, B. C., and McCaffery, C. (1994) Pseudosubstrate inhibition of CDPK, a protein kinase with a calmodulin-like domain, *Biochemistry 33*, 7278−7287.
10. Cheng, S. H., Willmann, M. R., Chen, H. C., and Sheen, J. (2002) Calcium signaling through protein kinases. The *Arabidopsis* calcium-dependent protein kinase gene family, *Plant Physiol. 129*, 469−485.
11. Fasano, J. M., Massa, G. D., and Gilroy, S. (2002) Ionic signaling in plant responses to gravity and touch, *J. Plant Growth Regul. 21*, 71−88.
12. Huber, S. C., Bachmann, M., and Huber, J. L. (1996) Post-translational regulation of nitrate reductase activity: a role for Ca^{2+} and 14-3-3 proteins, *Trends Plant Sci. 1*, 432−438.
13. Fu, H., Subramanian, R. R., and Masters, S. C. (2000) 14-3-3 proteins: structure, function, and regulation, *Annu. Rev. Pharmacol. Toxicol. 40*, 617−647.
14. Mackintosh, C. (2004) Dynamic interactions between 14-3-3 proteins and phosphoproteins regulate diverse cellular processes, *Biochem. J. 381*, 329−342.
15. Milne, F. C., Moorhead, G., Pozuelo Rubio, M., Wong, B., Kulma, A., Harthill, J. E., Villadsen, D., Cotelle, V., and MacKintosh, C. (2002) Affinity purification of diverse plant and human 14-3-3-binding partners, *Biochem. Soc. Trans. 30*, 379−381.
16. Pozuelo Rubio, M., Geraghty, K. M., Wong, B. H., Wood, N. T., Campbell, D. G., Morrice, N., and Mackintosh, C. (2004) 14-3-3-affinity purification of over 200 human phosphoproteins reveals new links to regulation of cellular metabolism, proliferation and trafficking, *Biochem. J. 379*, 395−408.

17. Yaffe, M. B. (2002) How do 14-3-3 proteins work? Gatekeeper phosphorylation and the molecular anvil hypothesis, *FEBS Lett. 513*, 53−57.
18. Aitken, A. (1995) 14-3-3 proteins on the MAP, *Trends Biochem. Sci. 20*, 95−97.
19. Emi, T., Kinoshita, T., and Shimazaki, K. (2001) Specific binding of vf14-3-3a isoform to the plasma membrane H^+-ATPase in response to blue light and fusicoccin in guard cells of broad bean, *Plant Physiol. 125*, 1115−1125.
20. Lu, G., Sehnke, P. C., and Ferl, R. J. (1994) Phosphorylation and calcium binding properties of an *Arabidopsis* GF14 brain protein homolog, *Plant Cell 6*, 501−510.
21. Fullone, M. R., Visconti, S., Marra, M., Fogliano, V., and Aducci, P. (1998) Fusicoccin effect on the in vitro interaction between plant 14-3-3 proteins and plasma membrane H^+-ATPase, *J. Biol. Chem. 273*, 7698−7702.
22. Bachmann, M., Huber, J. L., Athwal, G. S., Wu, K., Ferl, R. J., and Huber, S. C. (1996) 14-3-3 proteins associate with the regulatory phosphorylation site of spinach leaf nitrate reductase in an isoform-specific manner and reduce dephosphorylation of Ser-543 by endogenous protein phosphatases, *FEBS Lett. 398*, 26−30.
23. Athwal, G. S., Huber, J. L., and Huber, S. C. (1998) Biological significance of divalent metal ion binding to 14-3-3 proteins in relationship to nitrate reductase inactivation, *Plant Cell Physiol. 39*, 1065−1072.
24. Bachmann, M., Huber, J. L., Liao, P. C., Gage, D. A., and Huber, S. C. (1996) The inhibitor protein of phosphorylated nitrate reductase from spinach (*Spinacia oleracea*) leaves is a 14-3-3 protein, *FEBS Lett. 387*, 127−131.
25. Alsterfjord, M., Sehnke, P. C., Arkell, A., Larsson, H., Svennelid, F., Rosenquist, M., Ferl, R. J., Sommarin, M., and Larsson, C. (2004) Plasma membrane H(+)-ATPase and 14-3-3 isoforms of *Arabidopsis* leaves: evidence for isoform specificity in the 14-3-3/H(+)-ATPase interaction, *Plant Cell Physiol. 45*, 1202−1210.
26. Sehnke, P. C., DeLille, J. M., and Ferl, R. J. (2002) Consummating signal transduction: the role of 14-3-3 proteins in the completion of signal-induced transitions in protein activity, *Plant Cell 14* (Suppl.), S339−S354.
27. Sehnke, P. C., Rosenquist, M., Alsterfjord, M., DeLille, J., Sommarin, M., Larsson, C., and Ferl, R. J. (2002) Evolution and isoform specificity of plant 14-3-3 proteins, *Plant Mol. Biol. 50*, 1011−1018.
28. Otterhag, L., Gustavsson, N., Alsterfjord, M., Pical, C., Lehrach, H., Gobom, J., and Sommarin, M. (2006) *Arabidopsis* PDK1: identification of sites important for activity and downstream phosphorylation of S6 kinase, *Biochimie 88*, 11−21.
29. Babakov, A. V., Chelysheva, V. V., Klychnikov, O. I., Zorinyanz, S. E., Trofimova, M. S., and De Boer, A. H. (2000) Involvement of 14-3-3 proteins in the osmotic regulation of H^+-ATPase in plant plasma membranes, *Planta 211*, 446−448.
30. Fuglsang, A. T., Visconti, S., Drumm, K., Jahn, T., Stensballe, A., Mattei, B., Jensen, O. N., Aducci, P., and Palmgren, M. G. (1999) Binding of 14-3-3 protein to the plasma membrane H(+)-ATPase AHA2 involves the three C-terminal residues Tyr(946)-Thr-Val and requires phosphorylation of Thr(947), *J. Biol. Chem. 274*, 36774−36780.
31. Jahn, T., Fuglsang, A. T., Olsson, A., Bruntrup, I. M., Collinge, D. B., Volkmann, D., Sommarin, M., Palmgren, M. G., and Larsson, C. (1997) The 14-3-3 protein interacts directly with the C-terminal region of the plant plasma membrane H(+)-ATPase, *Plant Cell 9*, 1805−1814.
32. MacKintosh, C., and Meek, S. E. (2001) Regulation of plant NR activity by reversible phosphorylation, 14-3-3 proteins and proteolysis, *Cell. Mol. Life Sci. 58*, 205−214.
33. Muslin, A. J., Tanner, J. W., Allen, P. M., and Shaw, A. S. (1996) Interaction of 14-3-3 with signaling proteins is mediated by the recognition of phosphoserine, *Cell 84*, 889−897.
34. Yaffe, M. B., Rittinger, K., Volinia, S., Caron, P. R., Aitken, A., Leffers, H., Gamblin, S. J., Smerdon, S. J., and Cantley, L. C. (1997) The structural basis for 14-3-3:phosphopeptide binding specificity, *Cell 91*, 961−971.
35. Masters, S. C., Pederson, K. J., Zhang, L., Barbieri, J. T., and Fu, H. (1999) Interaction of 14-3-3 with a nonphosphorylated protein ligand, exoenzyme S of *Pseudomonas aeruginosa*, *Biochemistry 38*, 5216−5221.
36. Athwal, G. S., and Huber, S. C. (2002) Divalent cations and polyamines bind to loop 8 of 14-3-3 proteins, modulating their interaction with phosphorylated nitrate reductase, *Plant J. 29*, 119−129.
37. Athwal, G. S., Lombardo, C. R., Huber, J. L., Masters, S. C., Fu, H., and Huber, S. C. (2000) Modulation of 14-3-3 protein interactions with target polypeptides by physical and metabolic effectors, *Plant Cell Physiol. 41*, 523−533.
38. Athwal, G. S., Huber, J. L., and Huber, S. C. (1998) Phosphorylated nitrate reductase and 14-3-3 proteins. Site of interaction, effects of ions, and evidence for an AMP-binding site on 14-3-3 proteins, *Plant Physiol. 118*, 1041−1048.
39. Lu, G., DeLisle, A. J., de Vetten, N. C., and Ferl, R. J. (1992) Brain proteins in plants: an *Arabidopsis* homolog to neurotransmitter pathway activators is part of a DNA binding complex, *Proc. Natl. Acad. Sci. U.S.A. 89*, 11490−11494.
40. Lu, G., Rooney, M. F., Wu, K., and Ferl, R. J. (1994) Five cDNAs encoding *Arabidopsis* GF14 proteins, *Plant Physiol. 105*, 1459−1460.
41. Wu, K., Lu, G., Sehnke, P., and Ferl, R. J. (1997) The heterologous interactions among plant 14-3-3 proteins and identification of regions that are important for dimerization, *Arch. Biochem. Biophys. 339*, 2−8.
42. Wu, K., Rooney, M. F., and Ferl, R. J. (1997) The *Arabidopsis* 14-3-3 multigene family, *Plant Physiol. 114*, 1421−1431.
43. Shen, W., Clark, A. C., and Huber, S. C. (2003) The C-terminal tail of *Arabidopsis* 14-3-3omega functions as an autoinhibitor and may contain a tenth alpha-helix, *Plant J. 34*, 473−484.
44. Silhan, J., Obsilova, V., Vecer, J., Herman, P., Sulc, M., Teisinger, J., and Obsil, T. (2004) 14-3-3 protein C-terminal stretch occupies ligand binding groove and is displaced by phosphopeptide binding, *J. Biol. Chem. 279*, 49113−49119.
45. Truong, A. B., Masters, S. C., Yang, H., and Fu, H. (2002) Role of the 14-3-3 C-terminal loop in ligand interaction, *Proteins 49*, 321−325.
46. Liu, D., Bienkowska, J., Petosa, C., Collier, R. J., Fu, H., and Liddington, R. (1995) Crystal structure of the zeta isoform of the 14-3-3 protein, *Nature 376*, 191−194.
47. Pan, S., Sehnke, P. C., Ferl, R. J., and Gurley, W. B. (1999) Specific interactions with TBP and TFIIB in vitro suggest that 14-3-3 proteins may participate in the regulation of transcription when part of a DNA binding complex, *Plant Cell 11*, 1591−1602.
48. Wymer, C. L., Bibikova, T. N., and Gilroy, S. (1997) Cytoplasmic free calcium distributions during the development of root hairs of *Arabidopsis thaliana*, *Plant J. 12*, 427−439.
49. Paul, A. L., Sehnke, P. C., and Ferl, R. J. (2005) Isoform-specific subcellular localization among 14-3-3 proteins in *Arabidopsis* seems to be driven by client interactions, *Mol. Biol. Cell 16*, 1735−1743.
50. da Silva, E. F., Oliveira, V. H., Sorenson, M. M., Barrabin, H., and Scofano, H. M. (2002) Converting troponin C into calmodulin: effects of mutations in the central helix and of changes in temperature, *Int. J. Biochem. Cell Biol. 34*, 657−667.
51. Tikunova, S. B., Black, D. J., Johnson, J. D., and Davis, J. P. (2001) Modifying Mg^{2+} binding and exchange with the N-terminal of calmodulin, *Biochemistry 40*, 3348−3353.
52. Sinnige, M. P., Roobeek, I., Bunney, T. D., Visser, A. J., Mol, J. N., and de Boer, A. H. (2005) Single amino acid variation in barley 14-3-3 proteins leads to functional isoform specificity in the regulation of nitrate reductase, *Plant J. 44*, 1001−1009.
53. Sehnke, P. C., Laughner, B., Cardasis, H., Powell, D., and Ferl, R. J. (2006) Exposed loop domains of complexed 14-3-3 proteins contribute to structural diversity and functional specificity, *Plant Physiol. 140*, 647−660.
54. Yoon, G. M., Dowd, P. E., Gilroy, S., and McCubbin, A. G. (2006) Calcium-dependent protein kinase isoforms in petunia have distinct functions in pollen tube growth, including regulating polarity, *Plant Cell 18*, 867−878.
55. Legue, V., Blancaflor, E., Wymer, C., Perbal, G., Fantin, D., and Gilroy, S. (1997) Cytoplasmic free Ca^{2+} in *Arabidopsis* roots changes in response to touch but not gravity, *Plant Physiol. 114*, 789−800.
56. Wilker, E. W., Grant, R. A., Artim, S. C., and Yaffe, M. B. (2005) A structural basis for 14-3-3sigma functional specificity, *J. Biol. Chem. 280*, 18891−18898.

BI061366C